KSCE Journal of Civil Engineering (2020) 24(9):2824-2834
DOI 10.1007/s12205-020-0494-3

pISSN 1226-7988, eISSN 1976-3808
www.springer.com/12205

Water Resources and Hydrologic Engineering

Assessment of Inter-Model Variability in Meteorological Drought Characteristics Using CMIP5 GCMs over South Korea

Jang Hyun Sung[a], **Junehyeong Park**[b], **Jong-June Jeon**[c], **and Seung Beom Seo**[d]

[a]*Member, Ministry of Environment, Han River Flood Control Office, Seoul 06501, Korea*
[b]*Civil, Construction, and Environmental Engineering, University of Alabama, Tuscaloosa, AL 35487, USA*
[c]*Dept. of Statistics, University of Seoul, Seoul 02504, Korea*
[d]*Member, International School of Urban Sciences, University of Seoul, Seoul 02504, Korea*

ARTICLE HISTORY

Received 21 March 2019
Revised 1st 11 October 2019
Revised 2nd 16 April 2020
Accepted 22 April 2020
Published Online 14 July 2020

KEYWORDS

SPI
SPEI
GCM ensemble
Drought characteristics
Meteorological drought

ABSTRACT

Although many studies have sought to characterize future meteorological droughts, a few efforts have been done for quantifying the uncertainty, inter-model variability, arises from global circulation models (GCM) ensemble. A clear understanding of the uncertainty in multiple GCMs should be preceded before future meteorological droughts are projected. Therefore, this study evaluates the uncertainty in future meteorological drought characteristics that are induced by GCM ensemble using the custom measure "the degree of GCM spreading". Future meteorological drought indices, the standardized precipitation index (SPI) and standardized precipitation evapotranspiration index (SPEI), were computed to five different time scales: 3, 6, 9, 12 and 24 months using statistically downscaled 28 GCMs under Representative Concentration Pathway (RCP) 4.5 and 8.5 at 60 weather stations in South Korea. The frequency, duration, and severity of drought events were estimated for three different future periods; F1 (2010 – 2039), F2 (2040 – 2069), and F3 (2070 – 2099). It was found that the uncertainty increases as the time scale lengthens regardless of a choice of drought indices or RCP scenarios. It also turned out that the SPI exhibits larger uncertainty rather than the SPEI, because temperature data exhibit a relatively much smaller variability comparing to precipitation data. Moreover, there was a shift of regions having larger values of the increasing rate between F1 and F2, which is shift from the north-western to southern region of South Korea.

1. Introduction

Meteorological droughts are generally characterized by a dry weather patterns dominate an area, and the stipulated conditions vary across regions (Wilhite and Glantz, 1985). Meteorological droughts are interpreted as advance risk signals for agricultural and hydrological droughts. The occurrence of agricultural and hydrological droughts is accompanied by economic and social damage. It is therefore important to understand the characteristics of meteorological droughts and predict upcoming meteorological droughts. However, it is difficult to explain the direct link between meteorological droughts and risk to potential damages. For this reason, many researchers have proposed statistical indices to account for meteorological droughts such as standardized precipitation index (SPI) (Hayes et al., 1999), standardized precipitation evapotranspiration index (SPEI) (Vicente-Serrano et al., 2010), and Palmer drought index (PDSI) (Guttman, 1998). SPI quantifies precipitation as a standardized departure from a pre-defined probability distribution function that models the raw precipitation data (Keyantash, 2018). Unlike the SPI, the SPEI captures the main impact of increased temperatures on water demand (Vicente-Serrano et al., 2010). The SPEI uses the difference between the precipitation and PET. In addition, recent studies have analysed characteristics of meteorological droughts using the time series of the estimated drought indexes (e.g., Park et al., 2018; Sung et al., 2018a).

Moreover, projection of future meteorological droughts is a more challenging task. Hao et al. (2018) pointed out the remaining challenges to the projection of future droughts under changing climate and human-made environments. Improved physical models

CORRESPONDENCE Seung Beom Seo ✉ sbseo7@uos.ac.kr International School of Urban Sciences, University of Seoul, Seoul 02504, Korea

and merged statistical approaches (e.g., multi-model ensemble approaches) can be a potential solution for resolving the existing limitations. However, projecting future precipitation and temperature for the projection of droughts using global circulation models (GCMs) still implies huge uncertainty. This is because many different GCMs are provided and the likelihood of each GCM is also uncertain (IPCC, 2014). GCMs simulate the future weather conditions through physically rational mathematical equations. Nonetheless, the projection results can vary across GCMs due to their different boundary conditions and fundamental assumptions, therefore collecting the ensemble of GCM projections for the drought projection can lead to great uncertainty. For this reason, the characteristics of future meteorological droughts projected from multiple GCMs should be carefully interpreted. Nonetheless, during the past decade, studies have just projected future meteorological drought indices driven by future climate projections from multiple GCMs (e.g., Strzepek et al., 2010; Kirono et al., 2011; Liu et al., 2012; Jeong et al., 2014; Touma et al., 2015; Meresa et al., 2016). They have just presented how the droughts indices are estimated by applying multiple GCMs under different concentration-pathways (emission) scenarios without in-depth analyses on the projection results which vary across projection modelling chains. The projection modelling chain typically includes emission scenarios (concentration pathways), GCMs, downscaling methods, bias-correction schemes, (hydrologic) models (Seo et al., 2016).

As instantiated above, many studies have sought to characterize future meteorological droughts and similar efforts have been done for South Korea (e.g., Lee et al., 2015; Rhee and Cho, 2016; Jang, 2018). However, they overlooked that relative differences in uncertainty arises from various modelling chains for projection of future meteorological droughts using ensemble of GCMs. Thus, a clear understanding of uncertainty arises from various sources, such as a choice of drought index, time scale of the drought index, and future projection periods, should be preceded when the characteristics of future meteorological droughts are discussed. If the relative differences in uncertainty across various characteristics of future droughts are analysed, it can give us insight into the results of future drought projections. Therefore, the objective of this study is to evaluate the inter-model variability known as one source of uncertainties (Chen et al., 2014) in future meteorological drought characteristics that are induced by GCM ensemble. Furthermore, this study seeks for an appropriate drought index and time scales that are less sensitive to the uncertainty in future climate change.

This study uses statistically downscaled data sets of 28 GCMs under two RCP scenarios (RCP 4.5 and RCP 8.5) for 60 KMA ASOS weather stations. The two different drought indices, the SPI and SPEI, are calculated for meteorological droughts projections. The future meteorological drought is then characterized by the frequency, duration, and severity using the time series of the indices. The five different time scales (3, 6, 9, 12, and 24 months) are used for the both drought indices, and the indices are projected across three future periods, F1 (2010 – 2039), F2 (2040 – 2069), and F3 (2070 – 2099). That is, future drought projections are summarized by a three-dimensional drought characteristic vector, and there are 560 combinations (i.e., 2 drought indices × 5 time scales × 2 RCPs × 28 GCMs) of future drought projections for each future period and weather station. Inter-model variability of the GCMs are first analysed, and a spatial analysis based on weather stations are implemented.

2. Backgrounds

2.1 Data Collection and Input Data Construction

APEC Climate Center Integrated Modeling Solution (AIMS) provides precipitation and temperature data from Coupled Model Intercomparison Project Phase 5 (CMIP5) GCMs under RCP 4.5 and RCP 8.5 scenarios which are statistically downscaled to 60 locations of Korea Meteorological Administration automated surface observing system (KMA ASOS) weather stations in South Korea. Among the two statistical downscaling methods which are used in AIMS, this study downloaded the data sets applied by the spatial disaggregation with quantile delta mapping (SDQDM) method. SDQDM combines a spatial downscaling scheme based on inverse distance weighting method and a bias correction scheme that reflects long-term trends in climate change scenarios using empirical distributions (Eum and Cannon, 2017; Seo and Kim, 2018; Sung et al., 2018b; Kwon and Sung, 2019; Kwon et al., 2019; Seo et al., 2019b). In this study, 28 CMIP5 GCMs coupled with RCP 4.5 and 8.5 scenarios are spatially downscaled to 60 KMA ASOS stations and bias-corrected using observed climate data sets. The 28 GCMs used for this study are listed in Table 1, and the 60 KMA ASOS weather stations are presented in Fig. 1. Note that, since a single method for downscaling/bias-correction is applied, the variability of the downscaling/bias-correction method is not considered in this study.

2.2 Drought Indices

The two meteorological drought indices, the SPI and SPEI, are used for representing drought characteristics. The SPI is a widely applied index for characterizing meteorological drought on a range of timescales. It quantifies observed precipitation as a standardized departure from a selected probability distribution function that models the raw precipitation data (Keyantash, 2018). Thorn (1966) found the gamma distribution to fit well to climatological precipitation, but any extreme distribution function can be used if it is statistically suitable for the cumulative monthly precipitation. On the other hand, the SPEI is an extension of the SPI. The SPEI is designed to consider both precipitation and potential evapotranspiration (PET) in determining meteorological drought. Procedure and related formula for SPI computation are as below.

The gamma distribution is defined by its frequency or probability density function:

$$g(x) = \frac{1}{\beta^{\alpha}\Gamma(\alpha)} x^{\alpha-1} e^{-x/\beta} \tag{1}$$

Table 1. Description of CMIP5 GCMs Statistically Downscaled by Cho (2017) to KMA ASOS Weather Stations in South Korea

No.	GCMs	Atmospheric grid (Lat. × Lon., degree)	Institution
1	BCC-CSM1.1	2.7906 × 2.8125	Beijing Climate Center[1)]
2	BCC-CSM1.1(m)	2.7906 × 2.8125	
3	CanESM2	2.7906 × 2.8125	Canadian Centre for Climate Modelling and Analysis[2)]
4	CCSM4	0.9424 × 1.25	National Center for Atmospheric Research[3)]
5	CESM1(BGC)	0.9424 × 1.25	
6	CESM1(CAM5)	0.9424 × 1.25	
7	CMCC-CM	0.7484 × 0.75	Centro Euro-Mediterraneo sui Cambiamenti Climatici[4)]
8	CMCC-CMS	3.7111 × 3.75	
9	CNRM-CM5	1.4008 × 1.40625	Centre National de Recherches Meteorologiques[5)]
10	CSIRO-Mk3.6.0	1.8653 × 1.875	Commonwealth Scientific and Industrial Research Organization[6)]
11	FGOALS-g2	2.7906 × 2.8125	Institute of Atmospheric Physics[7)]
12	FGOALS-s2	1.6590 × 2.8125	
13	GFDL-ESM2G	2.0225 × 2	NOAA Geophysical Fluid Dynamics Laboratory[8)]
14	GFDL-ESM2M	2.0225 × 2.5	
15	HadGEM2-AO	1.25 × 1.875	Met Office Hadley Centre[9)]
16	HadGEM2-CC	1.25 × 1.875	
17	HadGEM2-ES	1.25 × 1.875	
18	INM-CM4	1.5 × 2	Institute for Numerical Mathematics[10)]
19	IPSL-CM5A-LR	1.8947 × 3.75	Institut Pierre-Simon Laplace[11)]
20	IPSL-CM5A-MR	1.2676 × 2.5	
21	IPSL-CM5B-LR	1.8947 × 3.75	
22	MIROC5	1.4008 × 1.40625	Atmosphere and Ocean Research Institute, The University of Tokyo[12)]; National Institute for Environmental Studies[13)]; Japan Agency for Marine-Earth Science and Technology[14)]
23	MIROC-ESM	2.7906 × 2.8125	
24	MIROC-ESM-CHEM	2.7906 × 2.8125	
25	MPI-ESM-LR	1.8653 × 1.875	Max Planck Institut fur Meteorologie[15)]
26	MPI-ESM-MR	1.8653 × 1.875	
27	MRI-CGCM3	1.12148 × 1.125	Meteorological Research Institute[16)]
28	NorESM1-M	1.8947 × 2.5	Norwegian Climate Centre[17)]

1) http://bcc.ncc-cma.net/; 2) https://www.canada.ca/en/environment-climate-change/services/climate-change/centre-modelling-analysis.html; 3) https://ncar.ucar.edu/; 4) https://www.cmcc.it/; 5) https://www.umr-cnrm.fr/; 6) https://www.csiro.au/; 7) http://english.iap.cas.cn/; 8) https://www.gfdl.noaa.gov/; 9) https://www.metoffice.gov.uk/; 10) http://www.inm.ras.ru/; 11) https://www.ipsl.fr/; 12) http://www.aori.u-tokyo.ac.jp/; 13) http://www.nies.go.jp/; 14) http://www.jamstec.go.jp/; 15) https://www.mpimet.mpg.de/; 16) http://www.mri-jma.go.jp/; 17) https://portal.enes.org/models/earthsystem-models/ncc/noresm

where $\alpha > 0$, α is a shape parameter, $\beta > 0$, β is a scale parameter.

$$\Gamma(\alpha) = \int_0^\infty x^{\alpha-1} e^{-x} \tag{2}$$

where $\Gamma(\alpha)$ is the gamma function.

The value of parameters α and β are then estimated by the maximum likelihood solutions:

$$\hat{\alpha} = \frac{1}{4A}\left(1 + \sqrt{1 + \frac{4A}{3}}\right) \tag{3}$$

$$\hat{\beta} = \frac{\bar{x}}{\alpha} \tag{4}$$

$$A = \ln\bar{x} - \frac{\sum \ln(x)}{n} \tag{5}$$

where n is the number of precipitation records.

The cumulative distribution function is then given by:

$$G(x) = \frac{1}{\Gamma(\hat{\alpha})}\int_0^x t^{\hat{\alpha}-1} e^{-t} dt \tag{6}$$

where $t = x/\hat{\beta}$.

The gamma function is undefined for $x = 0$ and a precipitation distribution may contain zeros (Shah et al., 2015), the cumulative probability becomes:

$$H(x) = q + (1-q)G(x) \tag{7}$$

where q is the probability of zero precipitation.

$H(x)$ is then transformed to the standard normal random variable, Z, with zero mean and standard deviance of one, which becomes the value of the SPI. SPI is generally categorized based on their range as presented in Table 2.

For SPEI computation, first, the difference between the

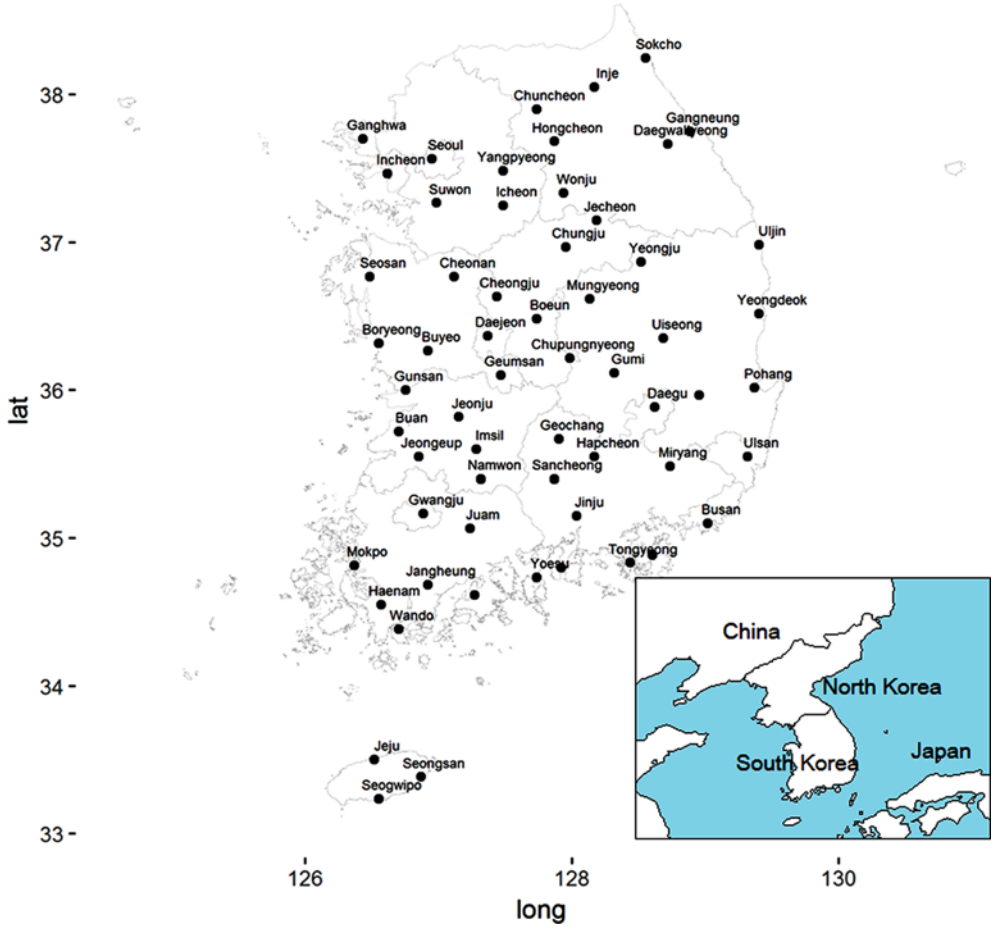

Fig. 1. Locations of 60 KMA ASOS Weather Stations Used for This Study

Table 2. Drought Categories from Range of SPI Values (McKee et al., 1993)

SPI	Drought categories
0 to -0.99	Mild drought
-1.00 to -1.49	Moderate drought
-1.50 to -1.99	Severe drought
-2.00 or less	Extreme drought

precipitation (P) and PET for the month i is calculated are as below:

$$D_i = P_i - PET_i \tag{8}$$

The calculated D_i values are then aggregated at different time scales. Vicente-Serrano et al. (2010) showed that the Log-logistic distribution provided better results than other distributions for obtaining SPEI series in standardized z units. The probability distribution function of a variable D according to the Log-logistic distribution is given by:

$$F(D) = \left[1 + \left(\frac{\alpha}{D-\gamma}\right)^{\beta}\right]^{-1} \tag{9}$$

where α, β, and γ are the scale, shape, and location parameters that are estimated by sample D.

Ahmad et al. (1988) discussed the L-moment procedure is the most robust and easy approach to obtain the Log-logistic parameters, α, β and γ. On the other hand, Vicente-Serrano et al. (2010) used the probability weighted moments (PWMs) method to calculate the parameter values, based on the plotting-position approach (Hosking, 1990a). Readers refer to the above references for details in the parameter estimation methods.

With $F(D)$, the SPEI can be easily obtained by standardizing the values of $F(D)$. For instance, following the traditional approximation equation of Abramowitz and Stegun (1965) can be used.

$$SPEI = W - \frac{C_0 + C_1 W + C_2 W^2}{1 + d_1 W + d_2 W^2 + d_3 W^3} \tag{10}$$

where, $W = -2\ln(P)$, P is the probability of exceeding a determined D value, i.e., $P = 1 - F(x)$ for $P \le 0.5$. The constants are C_0= 2.515517, C_1 = 0.802853, C_2 = 0.010328, d_1 = 1.432788, d_2 = 0.189269, d_3 = 0.001308.

Daily precipitation data from GCMs were aggregated to monthly scale for SPI calculation. For SPEI calculation, daily PET series were estimated first using daily precipitation and temperature data sets from GCMs. The values of PET were estimated with the simple Thornthwaite method (Thornthwaite, 1948) as suggested by Vicente-Serrano et al. (2010) due to its

simplicity of calculation and ease of data collection. Then, daily PET data were converted to monthly scale so that the difference between monthly precipitation and PET series can be calculated. The two drought indices, the SPI and SPEI, were calculated with five different time scales (3, 6, 9, 12, and 24 months), two RCP scenarios, 60 stations, 28 GCMs for three future periods.

2.3 Drought Characteristics

Using the calculated series of the indices, the drought characteristics are then specified by 1) frequency, 2) duration, and 3) severity. First, the frequency is calculated as the average number of drought events in the corresponding period as presented in Eq. (11). The duration is than calculated as the average length of the drought event as presented in Eq. (12). Finally, the severity is calculated as the average value of the drought index for a unit month across all drought events as presented in Eq. (13). Here, a negative value of the index-i.e., a drier condition comparing to the climatology-is considered as a drought condition, and a consecutive series of drought conditions-i.e., a series of negative values from its start to the end-is considered as a drought event.

$$frequency = \frac{M}{T} \tag{11}$$

$$duration = \frac{1}{M}\sum_{i=1}^{M} d_i \tag{12}$$

$$severity = \frac{1}{M}\sum_{i=1}^{M} v_i \tag{13}$$

where M is the number of drought events occurred during the planning horizon, T is the length (total number of months) of the planning horizon, d_i is the length of i^{th} drought event as shown in Fig. 2, v_i is the magnitude of i^{th} drought event that is defined as the sum of the values of the drought index in i^{th} drought event as shown in Fig.2.

2.4 Uncertainty Assessment

After calculating the drought indices for all combinations, the drought characteristic vectors - including frequency, duration, and severity – are estimated for 1,680 combinations (i.e., 2 drought indices × 5 time-scales × 2 RCPs × 28 GCMs × 3 future periods). Each drought characteristic vector is then normalized over the GCMs. The normalized vector of the k^{th} GCM is denoted by $u_k \in R^3$ where the notations for the other quantities are omitted for convenience. The set of the normalized vector, $\{u_k: k = 1, \ldots, 28\}$, can be analyzed on any criterion such as the drought index, weather station, RCP scenario, and future period. To assess the inter-model variability of the projected results, we use a following variability measure, 'the degree of GCM spreading' which defined as 'inter-model variability across all the GCMs' in this study. Since 'variance' is a measurement of the spread between values in a data set, 'inter-model variability across all the GCMs' should not be the same meaning of 'variability' of a single GCM.

$$\text{The degree of GCM spreading} = \sum_{k=1}^{28} \|u_k - \bar{u}\|_2 \tag{14}$$

where $\bar{u} = \sum_{k=1}^{28} u_k/28$ and $\| \ \|_2$ is an L2-norm operator (Golub and Van Loan, 1966). The above measure denotes the degree of GCM spreading in each drought index, weather station, RCP scenario, and future period. Besides, the measure is dimensionless so that the values of all situations can be compared. Ultimately, in this study, "the degree of GCM spreading" is defined as the uncertainty caused by multiple GCMs in the characteristics of future meteorological drought outlook.

Figure 3 explains how the climate projection ensemble transforms to the 'Degree of GCM spreading'. Excluding cases of stations (60 stations averaged), there are 1,680 climate projection ensemble (2 RCP × 28 GCMs × 3 future periods × 2 drought indices × 5 drought scales). All combinations above are possible from the data sets used in this research. Each drought index time-series has been estimated from each climate projection time-series, and each drought index time-series would have one value for frequency, duration, and vulnerability. Hence, total 1,680 values for frequencies, durations, and vulnerabilities are obtained. To know how they varies regardless of the amount of their values (the objective of this research is evaluating variabilities due to GCM ensemble, not future projection), these frequencies, durations, and vulnerabilities are standardized. Then, fixing RCP scenario, future period, and drought index on certain value respectively (e.g., RCP4.5, F1 period, and SPI12), it returns 28 values for GCMs. Each GCM have three values of F, D, and V as a form of vector. The sum of distance of 28 vectors from the mean vector of them is then defined as 'the degree of GCM spreading'.

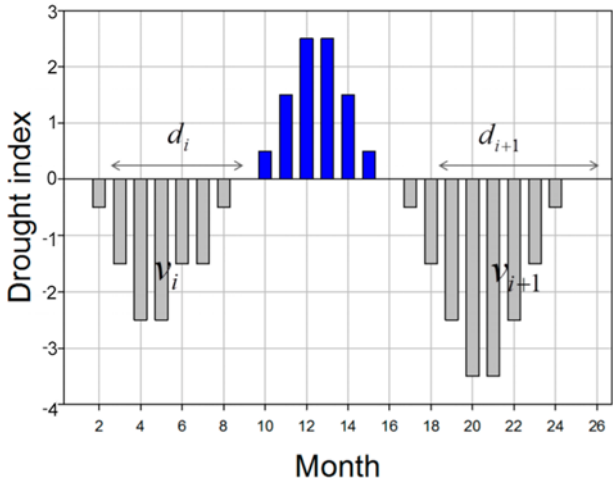

Fig. 2. Duration and Severity of Droughts Based on the Drought Threshold Level

3. Results

3.1 Analysis of Uncertainty in Future Drought Characteristics by GCM Ensemble

Uncertainty in future drought characteristics were analysed in terms of drought indices and different time scales. First, the values of 'the degree of GCM spreading' for drought characteristics

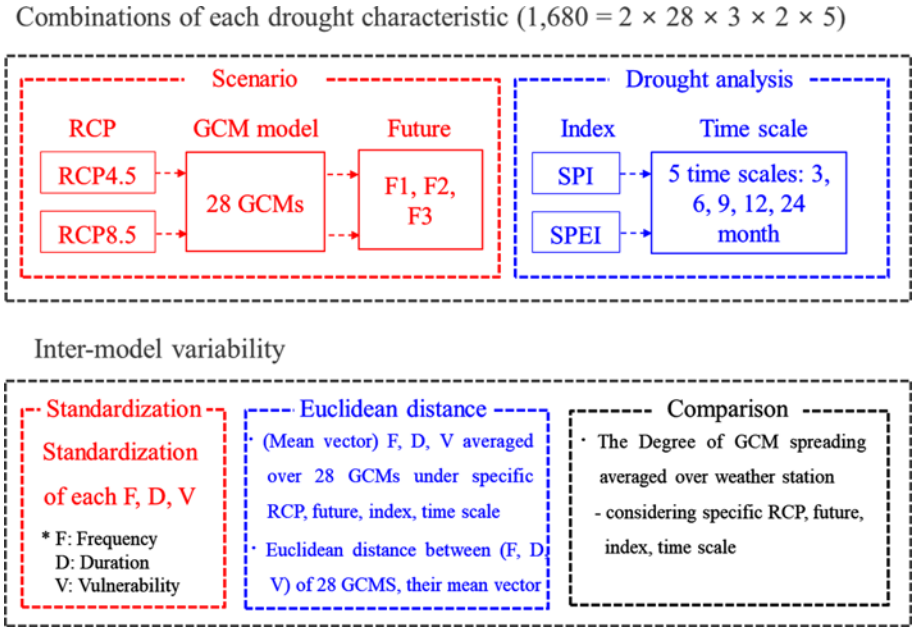

Fig. 3. Description of the Study

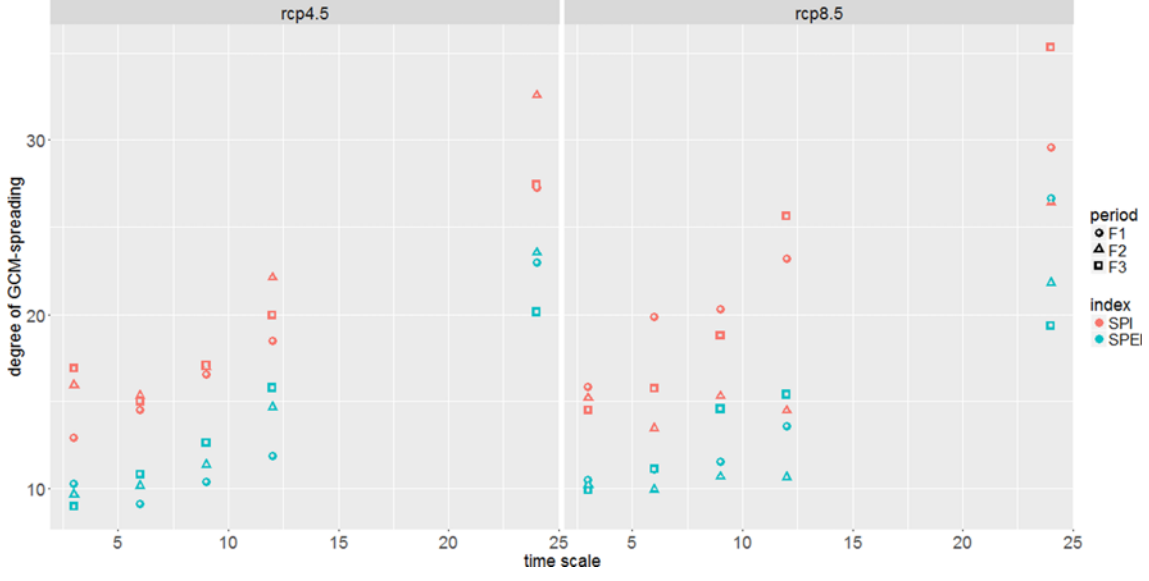

Fig. 4. Spatially Averaged Values of the Spread of Drought Characteristics for Five Different Time Scales and Two Drought Indices: (a) RCP 4.5, (b) RCP 8.5

(frequency, duration, severity) were averaged across all the weather stations. The spatially averaged values of "the degrees of GCM spreading" for each time scale, future period, and drought index are presented having different time scales of the indices in x-axis in Fig. 4. In addition, the same values presented having different future periods in x-axis in Fig. 5.

In Fig. 4, it is found that "the degrees of GCM spreading" is positively correlated with the time scale of the drought indices. In other words, inter-model variability across different GCMs increases as the time scale of the drought indices increases regardless of a choice of RCP scenario. The reason behind this finding is that GCM's capability of reproducing long-range dependency (LRD) of climate variables can vary a lot across different models. Seo et al. (2019a) discussed about GCM's inability to realize LRD inherent in climate. Therefore, it tells that uncertainty in future drought characteristics can increase when it is characterized by large time scale of drought indices. Besides, it is noteworthy that the SPI generally exhibits larger value of "the degrees of GCM spreading" than the SPEI. Since the SPI uses only precipitation whereas the SPEI utilizes the both precipitation and PET, it can be caused by that temperature data exhibit a relatively much smaller spread in comparison with precipitation data. This is clearly illustrated in Fig. 4 across all the different time scales.

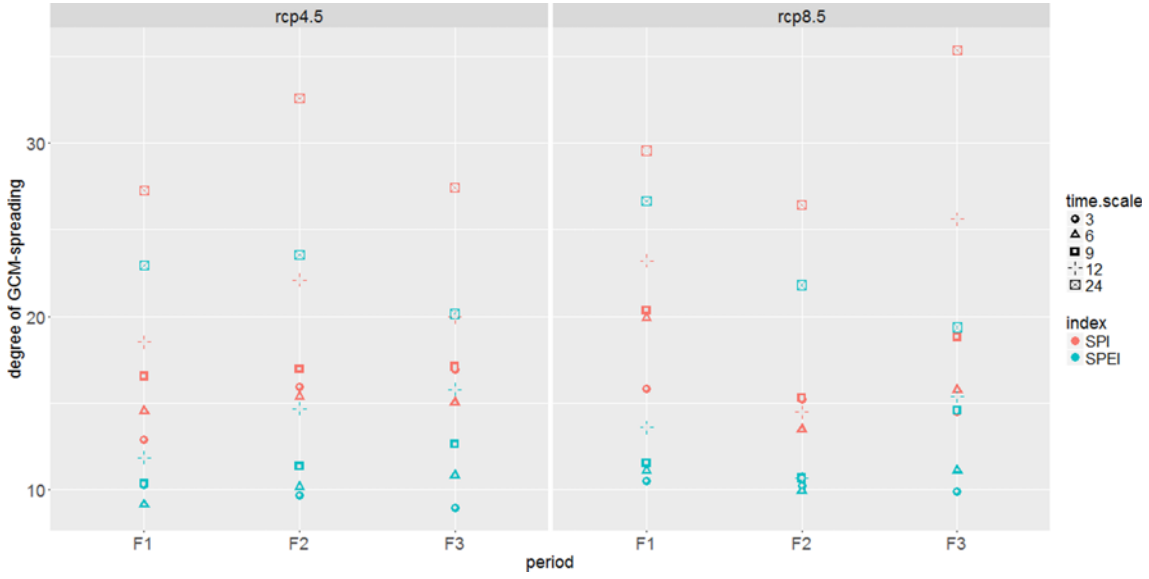

Fig. 5. Spatially Averaged Values of the Spread of Drought Characteristics for Three Different Future Periods: (a) RCP 4.5, (b) RCP 8.5

In Fig. 5, however, there is no significant trend in "the degrees of GCM spreading" over the future projection period. This finding contradicts the general idea that the greater uncertainty arises when longer-term future climate is projected. This might be because our analysis only evaluated inter-model variability across different GCMs rather than inherent uncertainty arises in GCM. Note that this study evaluated rather uncertainty in future drought characteristics (calculated from projected drought indices) than simple projection results of climate. Besides, there is no significant difference between RCP 4.5 and 8.5. Thus, it tells that a selection of GCMs and RCP scenario will not give significant impact on inter-model variability in future drought characteristics in each future period. The uncertainty of emission forcings is illustrated to be relatively minor (Hawkins and Sutton 2009). Conversely, the uncertainty related to natural climate variability appears the main source, especially for the monthly precipitation (Kim et al., 2016).

3.2 Spatial Distribution of Uncertainty in Future Drought Characteristics by GCM Ensemble

As discussed, there was a linear trend that 'the degree of GCM spreading' increases when drought scale increase as presented in Fig. 4. It infers that 'the degree of GCM spreading' increases as temporal scaled of drought index increase. Furthermore, in order to evaluate this trend on spatial domain, the spatial distribution of increase in "the degree of GCM spreading" is presented in Figs. 6 and 7 for RCP 4.5 and 8.5, respectively. Fixing RCP, future period, and drought index, each station has 5 degree of GCM spreading values for 5 different scale of drought index. Gradient colour represents increasing trend of "the degree of GCM spreading" across the time scale – i.e., a slope of a regression model – and the size of circle represents *p*-value. That is, Figs. 6 and 7 show the spatial differences of the rate which is the proportion of the changes in "the degree of GCM spreading" per unit increase in time scale of the drought indices.

The right column of Fig. 6 - i.e., Figs. 6(b), 6(d), and 6(f) - shows the results of the SPI under the RCP 4.5 scenario for F1, F2, and F3, respectively. It is interesting that there is a shift of regions having large value of the rate between F1 and F2, which is movement from the north-western to southern region of South Korea. On the other hand, the left column of Fig. 6 - i.e., Figs. 6(a), 6(c), and 6(e) - shows the results of the SPEI under the RCP 4.5 scenario. There is no significant difference between F1 and F2. Besides, the results between the SPI and SPEI are all similar regardless of future period.

Figure 7 presents the same with Fig. 6 but for RCP 8.5 scenario. Spatial regime shifts in Fig. 7 are similarly observed as the Fig. 6. Nonetheless, one difference is that there is strong signal on the northern region in F1 under RCP 8.5 scenario. However, the magnitudes of the rate are gradually decreased toward the longer lead time especially when it comes to the SPEI.

In most cases, a shift of regions having large value of the rate moves from the north-western region to the southern region over future period. This means that future drought characteristics of the north-western region should be carefully monitored in near future. On the other hand, future drought characteristics of the southern region should be carefully considered for longer future. Besides, there is difference between the results from the SPI and SPEI. In the case of the results from the SPEI, the linearly increasing trend of "the degree of GCM spreading" gets lessened with longer-term future period. Interestingly, it turns out that we need to pay more attention to the drought outlooks for near-term future because uncertainty in drought characteristics caused by GCM ensemble is very sensitive to a choice of time scale of the drought indices in near future.

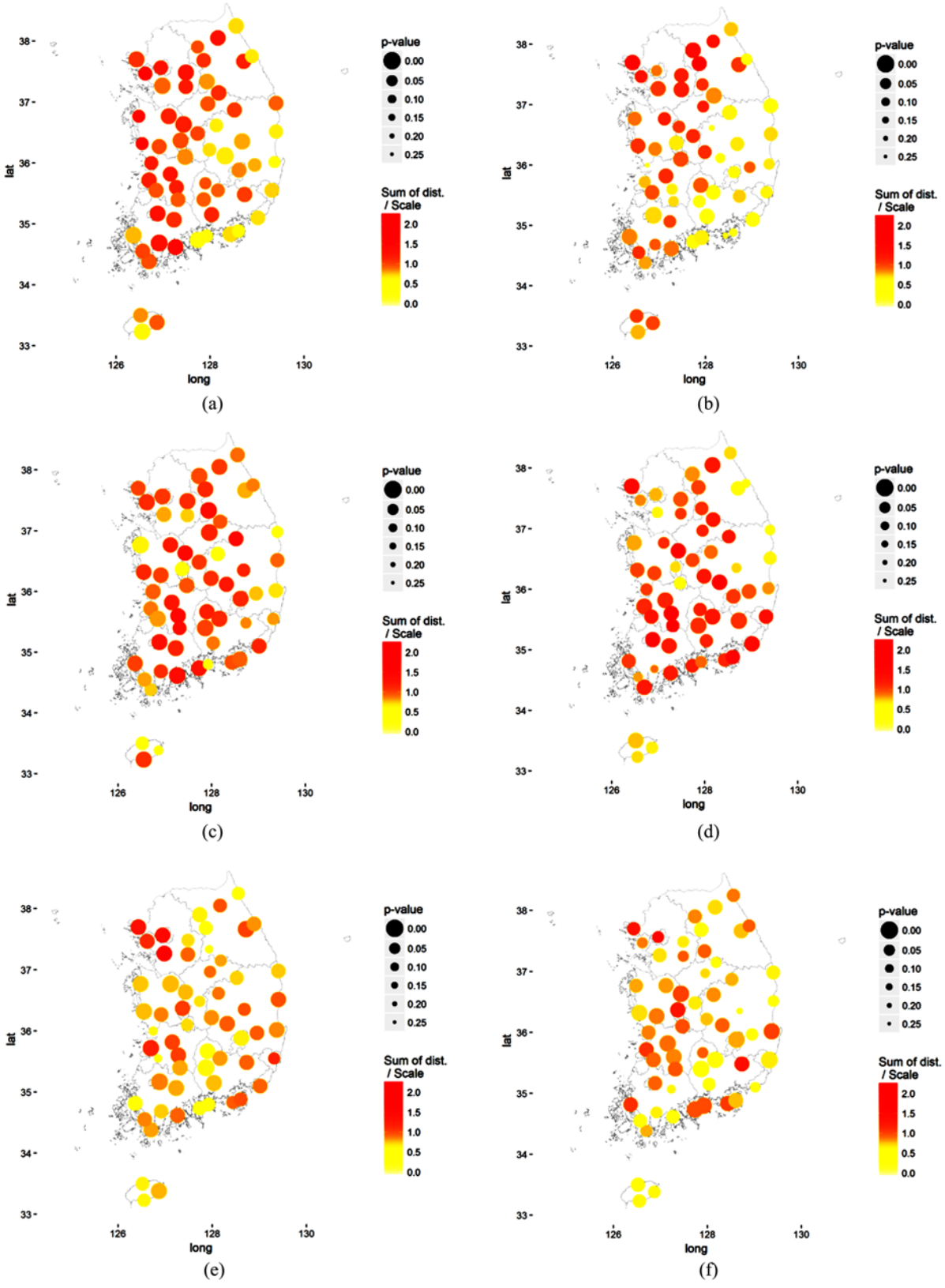

Fig. 6. Spatial Distribution of the Increasing Rate of the Spread of Drought Characteristics: (a) SPEI – RCP 4.5 – F1, (b) SPI – RCP 4.5 – F1, (c) SPEI – RCP 4.5 – F2, (d) SPI – RCP 4.5 – F2, (e) SPEI – RCP 4.5 – F3, (f) SPI – RCP 4.5 – F3

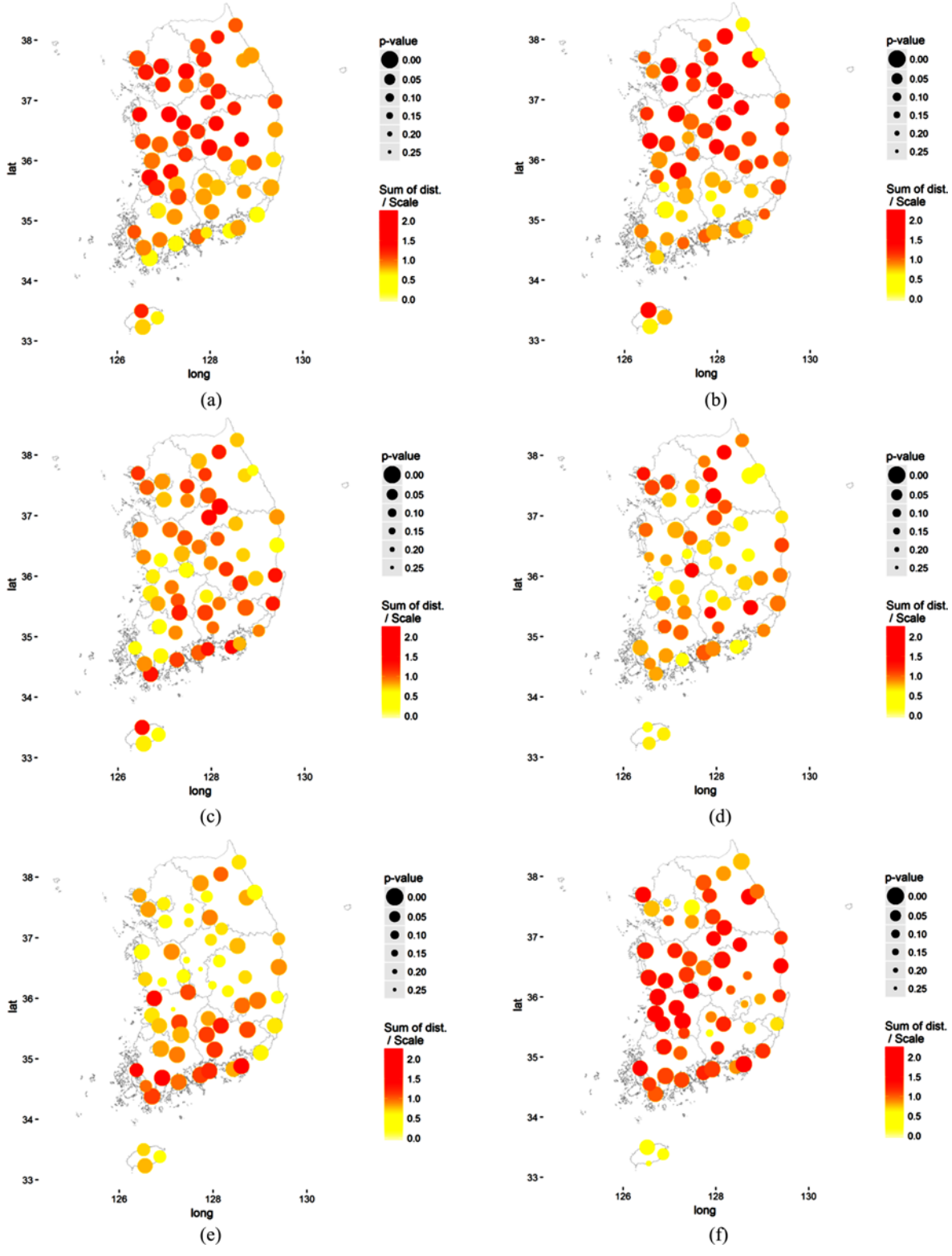

Fig. 7. Spatial Distribution of the Increasing Rate of the Spread of Drought Characteristics: (a) SPEI – RCP 8.5 – F1, (b) SPI – RCP 8.5 – F1, (c) SPEI – RCP 8.5 – F2, (d) SPI – RCP 8.5 – F2, (e) SPEI – RCP 8.5 – F3, (f) SPI – RCP 8.5 – F3

4. Conclusions

In this study, uncertainties in future meteorological drought characteristics caused by CMIP5 multiple GCMs were analysed using the custom measure "the degree of GCM spreading". Future meteorological drought was projected using 28 GCMs under RCP 4.5 and 8.5, which were statistically downscaled at 60 KMA ASOS weather stations. Two meteorological drought

indices, the SPI and SPEI, were calculated with five different time scales: 3, 6, 9, 12 and 24 months. The frequency, duration, and severity of drought events were estimated for three different future periods: F1, F2, and F3. The inter-model variability of future drought characteristics, which is defined as "the degree of GCM spreading" in this study, was calculated to evaluate the impacts of the GCM ensemble on uncertainty in future drought characteristics. Based on the results of "the degree of GCM spreading", the appropriate drought index and corresponding time scale were discussed to determine proper drought index and time scale which are less affected by uncertainties caused by GCM ensemble.

As a result of "The degree of GCM spreading" in terms of the time scale of the drought index, the inter-model variability increases as the time scale of the drought index lengthened, regardless of drought indices or RCP scenarios. It can be induced that GCM's capability of realizing long-range dependency (LRD) of climate variables can lead to huge uncertainty in longer time scale of drought indices. Besides, it also turns out that the SPI exhibits larger uncertainty rather than the SPEI, because temperature data exhibit a relatively much smaller variability comparing to precipitation data. On the other hand, the inter-model variability does not significantly change across different future periods.

Moreover, the uncertainty in future drought characteristics caused by GCM ensemble was spatially investigated in terms of the time scale of the drought indices. Overall, there was a shift of regions having large value of the increasing rate between F1 and F2, which is shift from the north-western to southern region of South Korea. In addition, in case of the SPEI, the increasing trend of the uncertainty in future drought characteristics lessened with longer-term future period.

The findings of this study deliver a message that we should carefully select the drought index and its time scale especially for near-term future. Along with the inability of GCMs in reproducing LRD, huge seasonal variability of climate variables also can lead to huge uncertainty in future drought outlooks. When longer time scale of the drought index is considered – e.g., longer than 12 months – entire seasonality of climate variables affects the estimation of the indices. In other words, the wet seasons are added to the moving window of the indices (Park et al., 2017). It should be noted that the huge seasonality of climate variable is also a potential source of uncertainty in drought projection. However, it would be beyond of this study, which can be implemented as a following study. The authors also concern about that only meteorological drought characteristics were analysed in this study. It might return different results if hydrological drought indices which are estimated by streamflow series are utilized because they are affected by localized hydrological process.

Acknowledgements

This research has been supported by a grant NRF-2016R1C1B1010545 funded by the Ministry of Science, ICT and Future Planning. The authors also thank for University of Seoul for their support.

ORCID

Junehyeong Park https://orcid.org/0000-0001-7806-4803
Jong-June Jeon https://orcid.org/0000-0002-1423-4292
Seung Beom Seo https://orcid.org/0000-0001-9819-6555

References

Abramowitz M, Stegun IA (1965) Handbook of mathematical functions: With formulas, graphs, and mathematical tables. US Department of Commerce, National Bureau of Standards, Gaithersburg, MD, USA

Ahmad MI, Sinclair CD, Werritty A (1988) Log-logistic flood frequency analysis. *Journal of Hydrology* 98:205-224, DOI: 10.1016/0022-1694(88)90015-7

Chen H, Sun J, Chen X (2014) Projection and uncertainty analysis of global precipitation-related extremes using CMIP5 models. *International Journal of Climatology* 34(8):2730-2748, DOI: 10.1002/joc.3871

Cho J, Chung I, Jo W, Kang D, Lee J (2017) Downscaled climate change scenarios data for Korean Peninsula. APEC Climate Center, Busan, Korea

Eum H-I, Cannon AJ (2017) Intercomparison of projected changes in climate extremes for South Korea: Application of trend preserving statistical downscaling methods to the CMIP5 ensemble. *International Journal of Climatology* 37(8):3381-3397, DOI: 10.1002/joc.4924

Golub GH, Van Loan CF (1996) Matrix computations, 3rd edition. Johns Hopkins, Baltimore, MD, USA

Guttman NB (1998) Comparing the palmer drought index and the Standardized Precipitation Index. *Journal of the American Water Resources Association* 34(1):113-121, DOI: 10.1111/j.1752-1688.1998.tb05964.x

Hao Z, Singh VP, Xia Y (2018) Seasonal drought prediction: Advances, challenges, and future prospects. *Review of Geophysics* 56(1):108-141, DOI: 10.1002/2016RG000549

Hawkins E, Sutton R (2009) The potential to narrow uncertainty in regional climate predictions. *Bulletin of the American Meteorological Society* 90(8):1095-1108, DOI: 10.1175/2009BAMS2607.1

Hayes M, Wilhite DA, Svoboda M, Vanyarkho V (1999) Monitoring the 1996 drought using the Standardized Precipitation Index. *Bulletin of the American Meteorological Society* 80(3):429-438, DOI: 10.1175/1520-0477(1999)080<0429:MTDUTS>2.0.CO;2

Hosking JRM (1990) L-moments: Analysis and estimation of distributions using linear combinations of order statistics. *Journal of the Royal Statistical Society: Series B (Methodological)* 52(1):105-124, DOI: 10.1111/j.2517-6161.1990.tb01775.x

IPCC (2014) Climate change 2014: Impacts, adaptation, and vulnerability. Intergovernmental Panel on Climate Change, Working Group II, Cambridge University Press, Cambridge, UK

Jang D (2018) Assessment of meteorological drought indices in Korea using RCP 8.5 scenario. *Water* 10(3):283, DOI: 10.3390/w10030283

Jeong DI, Sushama L, Khaliq MN (2014) The role of temperature in drought projections over North America. *Climatic Change* 127(2):289-303, DOI: 10.1007/s10584-014-1248-3

Keyantash K (2018) The climate data guide: Standardized precipitation index (SPI). Climate Data Guide, Retrieved March 10, 2019, https://climatedataguide.ucar.edu/climate-data/standardized-precipitation-index-

spi

Kim J, Ivanov VY, Fatichi S (2016) Climate change and uncertainty assessment over a hydroclimatic transect of Michigan. *Stochastic Environment Research and Risk Assessment* 30:923-944, DOI: 10.1007/s00477-015-1097-2

Kirono DGC, Kent DM, Hennessy KJ, Mpelasoka F (2011) Characteristics of Australian droughts under enhanced greenhouse conditions: Results from 14 global climate models. *Journal of Arid Environments* 75(6):566-575, DOI: 10.1016/j.jaridenv.2010.12.012

Kwon M, Sung JH (2019) Changes in future drought with HadGEM2-AO Projections. *Water* 11(2):312, DOI: 10.3390/w11020312

Kwon M, Sung JH, Ahn J (2019) Change in extreme precipitation over North Korea using multiple climate change scenarios. *Water* 11(2):270, DOI: 10.3390/w11020270

Lee J-H, Jang H-W, Kim J-S, Kim T-W (2015) Quantitative characterization of historical drought events in Korea – Focusing on drought frequency analysis in the five major basins. *Journal of Korean Water Resources Association* 48(12):1011-1021, DOI: 10.3741/JKWRA.2015.48.12.1011

Liu L, Hong Y, Bednarczyk CN, Yong B, Shafer MA, Riley R, Hocker JE (2012) Hydro-climatological drought analyses and projections using meteorological and hydrological drought indices: A case study in Blue River basin, Oklahoma. *Water Resources Management* 26(10):2761-2779, DOI: 10.1007/s11269-012-0044-y

McKee TB, Doesken NJ, Kleist J (1993) The relationship of drought frequency and duration to time scales. *8th Conference on Applied Climatology* 17(22):179-183

Meresa H, Osuch M, Romanowicz R (2016) Hydro-meteorological drought projections into the 21st century for selected Polish catchments. *Water* 8(5):206, DOI: 10.3390/w8050206

Park J, Cho J, Lee E-J, Jung I (2017) Evaluation of reference evapotranspiration in South Korea according to CMIP5 GCMs and estimation methods. *Journal of the Korean Society of Rural Planning* 23(4):153-168, DOI: 10.7851/Ksrp.2017.23.4.153 (in Korean)

Park J-H, Lim YJ, Kim BJ, Sung JH (2018) Appraisal of drought characteristics of representative drought indices using meteorological variables. *KSCE Journal of Civil Engineering* 22(7):2002-2009, DOI: 10.1007/s12205-018-2744-1

Rhee J, Cho J (2016) Future changes in drought characteristics: Regional analysis for South Korea under CMIP5 projections. *Journal of Hydrometeorology* 17(1):437-451, DOI: 10.1175/JHM-D-15-0027.1

Seo SB, Kim Y-O (2018) Impact of spatial aggregation level of climate indicators on a national-level selection for representative climate change scenarios. *Sustainability* 10(7):2409, DOI: 10.3390/su10072409

Seo SB, Kim Y-O, Kang S-U (2019a) Time-varying discrete hedging rules for drought contingency plan considering long range dependency in streamflow. *Water Resources Management* 33(6):2791-2807, DOI: 10.1007/s11269-019-02244-5

Seo SB, Kim Y-O, Kim Y, Eum H-I (2019b) Selecting climate change scenarios for regional hydrologic impact studies based on climate extremes indices. *Climate Dynamics* 52(2):1595-1611, DOI: 10.1007/s00382-018-4210-7

Seo SB, Sinha T, Mahinthakumar G, Sankarasubramanian A, Kumar M (2016) Identification of dominant source of errors in developing streamflow and groundwater projections under near-term climate change. *Journal of Geophysical Research – Atmosphere* 121(13):7652-7622, DOI: 10.1002/2016JD025138

Shah R, Bharadiya N, Manekar V (2015) Drought index computation using standardized precipitation index (SPI) method for Surat District, Gujarat. *Aquatic Procedia* 4:1243-1249, DOI: 10.1016/j.aqpro.2015.02.162

Strzepek K, Yohe G, Neumann J, Boehlert B (2010) Characterizing changes in drought risk for the United States from climate change. *Environmental Research Letters* 5:044012, DOI: 10.1088/1748-9326/5/4/044012

Sung JH, Chung E, Shahid S (2018a) Reliability-resiliency-vulnerability approach for drought analysis in South Korea using 28 GCMs. *Sustainability* 10(9):3043, DOI: 10.3390/su10093043

Sung JH, Eum H-I, Park J, Cho J (2018b) Assessment of climate change impacts on extreme precipitation events: Applications of CMIP5 climate projections statistically downscaled over South Korea. *Advances in Meteorology* 02018:4720523, DOI: 10.1155/2018/4720523

Thorn HCS (1966) Some methods of climatological analysis. WMO Technical Note No.81, World Meteorological Organization, Geneva, Switzerland, 16-22

Thornthwaite CW (1948) An approach toward a rational classification of climate. *Geographical Review* 38(1):55-94, DOI: 10.2307/210739

Touma D, Ashfaq M, Nayak MA, Kao S-C, Diffenbaugh NS (2015) A multi-model and multi-index evaluation of drought characteristics in the 21st century. *Journal of Hydrology* 526:197-207, DOI: 10.1016/j.jhydrol.2014.12.011

Vicente-Serrano SM, Begueria S, Lopez-Moreno JI (2010) A multiscalar drought index sensitive to global warming: The standardized precipitation evapotranspiration index. *Journal of Climate* 23(7):1696-1718, DOI: 10.1175/2009JCLI2909.1

Wilhite DA, Glantz MH (1985) Understanding the drought phenomenon: The role of definitions. *Water International* 10(3):111-120, DOI: 10.1080/02508068508686328